International Journal of Electrical, Electronic and Communication Sciences
ISSN: 2517-9438
Vol:8, No:7, 2014

Hysteresis Control of Power Conditioning Unit for Fuel Cell Distributed Generation System

Kanhu Charan Bhuyan, Subhransu Padhee, Rajesh Kumar Patjoshi, Kamalakanta Mahapatra

Abstract—Fuel cell is an emerging technology in the field of renewable energy sources which has the capacity to replace conventional energy generation sources. Fuel cell utilizes hydrogen energy to produce electricity. The electricity generated by the fuel cell can't be directly used for a specific application as it needs proper power conditioning. Moreover, the output power fluctuates with different operating conditions. To get a stable output power at an economic rate, power conditioning circuit is essential for fuel cell. This paper implements a two-staged power conditioning unit for fuel cell based distributed generation using hysteresis current control technique.

Keywords—Fuel cell, power conditioning unit, hysteresis control.

I. Introduction

THE increasing demand of energy and limited supply of fossil fuel has forced mankind to search for alternate medium to meet its energy demand. Renewable energy sources such as wind, solar, hydro power, biomass and hydrogen are emerging as potential solution for environmental friendly power generation system.

From the above mentioned renewable energy sources, hydrogen is one of the simplest and easily available material in atmosphere. Recently hydrogen energy is widely used as fuel and energy source. Fuel cell utilizes the chemical reaction between hydrogen and oxygen to produce electric power. The conversion of chemical process to electrical energy doesnot emit any toxic gases as by products. Fuel cell can be treated as a battery but the fuel cell doesnot have any charging time unlike the battery and has high power density and power conversion efficiency. As fuel cell provides a clean renewable energy, many countries are trying to utilize this technique as a potential source of energy generation.

Distributed generation system powered by different renewable energy sources (micro-sources) have been gaining widespread acceptance because of higher efficiency, higher reliability and low cost. Among different micro-sources, fuel cell is widely used because of its high efficiency and modular structure. Fuel cell based distributed generation system generates electric power, which is subsequently injected in to the distributed power system. In [1], PEMFC distributed generation system is reported. The fuel cell is interfaced with the grid using DC-DC boost converter and 3-ϕ PWM-VSI. Hysteresis controller based energy harvesting technique for microbial fuel cell (MFC) is discussed in [2]. The performance of fuel cell distributed generation system against voltage sag is reported in [3]. Considering the nonlinearities involved in distributed generation system, P. Sekhar et.al [4], proposed a sliding mode based feedback linearization controller for grid connected fuel cell distributed generation system. A novel power electronic interface is proposed in [5]. In this proposed topology, a voltage doubler circuit is used in the boost converter to achieve higher level of voltage. Researchers have also used artificial intelligent techniques like fuzzy logic for grid integration of fuel cell [6].

Fuel cell generates a low voltage DC power and gives a sluggish response to a sudden change in load. So energy storage units (batteries, ultra capacitors) are used. To compensate for the sluggish response and provide utility AC power, some form of power conditioner is required. Therefore, a power conditioning unit (PCU) is used along with fuel cell stack. According to the number of power electronic converter, PCU can be broadly classified as two-staged PCU and single staged PCU. In two-staged PCU, a DC-DC converter is used to step up the raw DC voltage produced by the fuel cell and then a DC-AC inverter converts the DC voltage to AC voltage. In single staged PCU, only a DC-AC inverter is used to convert the fuel cell voltage to AC power. This paper concentrates on two staged PCU because the primary limitation of single stage PCU is the high current flow in inverter and primary side of the step-up transformer [7].

When interfaced with the utility grid, the fuel cell has to provide a stable output despite change in load profile. So design of PCU and design of an appropriate controller for PCU is also important. In the fuel cell distributed generation system, dynamics of each and every components has to be modelled. This paper presents an overall design and simulation results for a fuel cell distributed generation system. The fuel cell is connected with the grid via a multi-staged PCU. The multi staged PCU consists of DC-DC boost converter and 3-ϕ inverter. LC filter and interfacing inductors are used for grid synchronization and to provide a ripple free output. The dynamics of fuel cell and associated power electronic converters are modelled. Hysteresis control is used to control the PCU because this particular control strategy is simple yet robust and efficiently compensates for different disturbances in the load profile. A simulation model of the distributed generation system is developed and it is shown that the fuel cell based distributed generation system performs according to the desired specifications.

Kanhu Charan Bhuyan is with the Department of Instrumentation and Electronics Engineering, College of Engineering and Technology, Bhubaneswar, Odisha, India, (e-mail: kanhu2006@gmail.com).

Subhransu Padhee, Rajesh Kumar Patjoshi and Kamalakanta Mahapatra are with Department of Electronics and Communication Engineering, National Institute of Technology, Rourkela, Odisha, India (e-mail: subhransupadhee@gmail.com,rajeshpatjoshi1@gmail.com,kkm@nitrkl.ac.in).

II. Modeling of Fuel Cell

Fuel cell consists of an electrolyte layer which is in contact with two electrodes, one fuelled with hydrogen (anode) and the other with oxygen (cathode). The electrolyte which acts like a membrane permits only the positive ions to flow from anode to cathode and acts as an insulator for electrons. The electron produced from the hydrogen fuel electrode after decomposition tries to get stable by going to cathode side which is accomplished by an external circuit and this way, electricity is generated. According to the type of electrolyte and operating temperature, fuel cell can be classified in to five different types such as (a) Direct methanol fuel cell, (b) Proton exchange membrane fuel cell, (c) Alkaline fuel cell, (d) Molten carbon fuel cell and (e) Solid oxide fuel cell.

This paper considers solid oxide fuel cell (SOFC) because it works at a high temperature and is ideal for use in distributed generation system [4]. Transient and static characteristics of fuel cell is discussed in [8], [9] whereas the modeling of SOFC for power system dynamics is proposed in [10], [11]. A review of SOFC modelling can be found in [12]–[15].

In a fuel cell, the electrochemical oxidation of hydrogen takes place in anode side and can be represented according to (1). The cathode side of the reaction can be represented as (2) and the overall electrochemical reaction of fuel cell can be represented as (3) .

$$H_2 \rightarrow 2H^+ + 2e^- \tag{1}$$

$$\tfrac{1}{2}O_2 + 2H^+ + 2e^- \rightarrow H_2O \tag{2}$$

$$H_2 + \tfrac{1}{2}O_2 \rightarrow H_2O \tag{3}$$

The utilization factor of a fuel cell is defined as the ratio between the fuel flow that reacts and the fuel injected to the stack and can be represented as (4) .

$$U_f = \frac{q^{in}_{H_2} - q^{out}_{H_2}}{q^{in}_{H_2}} = \frac{q^{r}_{H_2}}{q^{in}_{H_2}} \tag{4}$$

U_f is the utilization factor and q_{H_2} is the molar flow of hydrogen.

The performance of fuel cell is characterized by the polarization curve (V-I characteristics curve) of fuel cell. The above mentioned reactions release electrons and build up difference of potential energy between two terminals (cathode and anode). The potential difference at no load condition is called open circuit voltage or Nernst voltage which can be represented as

$$V_{open} = N_o\left[V_o + \frac{RT}{2F}\ln\left(\frac{P_{H_2}\sqrt{P_{O_2}}}{P_{H_2O}}\right)\right] \tag{5}$$

where, V_{open} is the open circuit voltage or Nernst voltage at no load condition, N_o is the number of cells connected in series, T is the Operating Temperature of fuel cell (Kelvin), F is the Faraday Constant (96486 C/mol), R is the Universal Gas Constant (8.314 $kJ/kmol.K$) and V_o = 1.1 V is the standard potential. Partial pressure of oxygen, hydrogen and water is represented as P_{H_2}, P_{O_2} and P_{H_2O} respectively and can be obtained from the following differential equations.

$$\dot{P}_{H_2} = -\frac{1}{t_{H_2}}\left(P_{H_2} + \frac{1}{K_{H_2}}\left(q^{in}_{H_2} - 2K_rI_{fc}\right)\right) \tag{6}$$

$$\dot{P}_{O_2} = -\frac{1}{t_{O_2}}\left(P_{O_2} + \frac{1}{K_{O_2}}\left(q^{in}_{O_2} - 2K_rI_{fc}\right)\right) \tag{7}$$

$$\dot{P}_{H_2O} = -\frac{1}{t_{H_2O}}\left(P_{H_2O} + \frac{2}{K_{H_2O}}K_rI_{fc}\right) \tag{8}$$

Here K_r is a constant and I_{fc} is current of fuel cell stack.

There are different losses in the fuel cell and considering all the losses, the output voltage of single fuel cell can be defined as

$$V_{FC} = V_{open} - V_{ohm} - V_{act} - V_{conc} \tag{9}$$

V_{act} is the voltage loss due to rate of reactions on the surface of the electrodes, V_{ohm} is the Ohmic voltage drop from the resistances of proton flow in the electrolyte and V_{conc} is the loss in concentration.

$$V_{ohm} = NI_{fc}R_{ohm} \tag{10}$$

$$V_{act} = N_o\left(\frac{RT}{2\alpha F}\right)\ln\left(\frac{I_{fc} + I_n}{I_o}\right) \tag{11}$$

$$V_{conc} = Nm\exp\left(nI_{fc}\right) \tag{12}$$

I_n is the internal current density, I_{fc} is the fuel cell current, α is the charge transfer coefficient.

To create a fuel cell stack, n number of fuel cell is connected in series. The output voltage of fuel cell stack is represented as

$$V_s = nV_{FC} \tag{13}$$

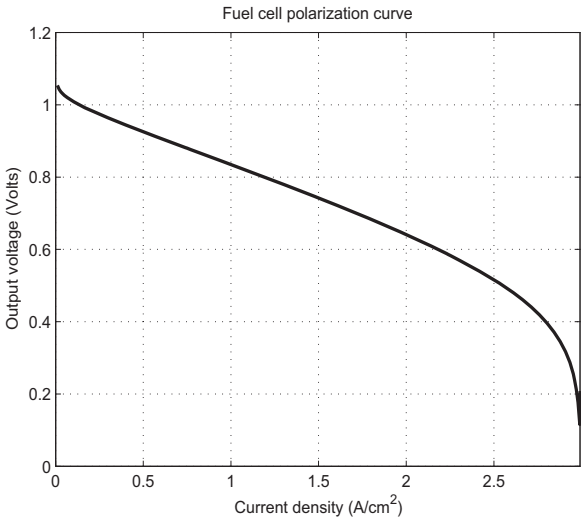

Fig. 1. Simulated polarization curve of fuel cell

Fig. 1 shows the simulation results of cell voltage versus current density characteristic of a typical fuel cell. It can be

seen that when the current increases, there is voltage drop. The drop is because of the activation loss. In the voltage drop, a linear region exists which is due to the ohmic loss. In the final stages the voltage drops sharply to zero when the current density is maximum. The sharp drop in voltage is attributed to concentration loss in fuel cell.

III. Power Conditioning Unit

The unregulated output DC voltage of fuel cell stack has to be conditioned by a power conditioning unit (PCU). There are numerous topologies of PCU available. The review of different topologies of PCU for grid integration of renewable energy sources can be found in [16]–[19]. The control and grid synchronization of distributed power generation system is reported in [20]. The complete block diagram of hysteresis control of PCU for fuel cell distributed generation system is shown in Fig. 2.

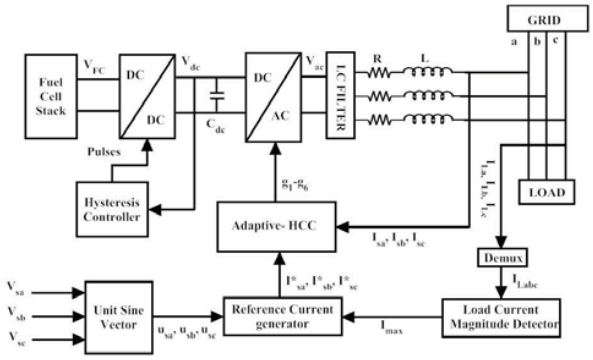

Fig. 2. Block diagram of PCU for fuel cell distributed generation system

A. DC-DC Boost Converter

DC-DC converter are light weight, efficient power conversion device which are widely used in many applications. Though there are different topologies of DC-DC converter, the basic converter used to step up the input voltage is Boost converter. This paper assumes the converter operating in continuous conduction mode (CCM) with switching period T and duty cycle d. The power circuit of DC-DC boost converter is shown in Fig. 3. The state space average model of DC-DC

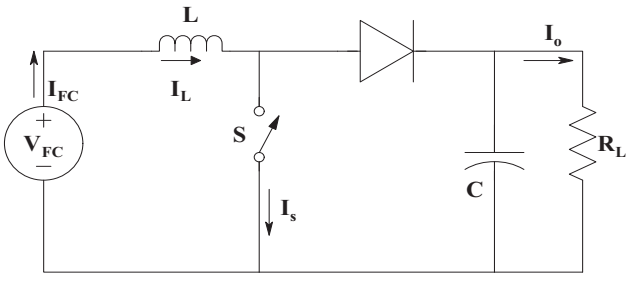

Fig. 3. DC-DC Boost Converter

boost converter is represented as

$$\begin{bmatrix} \dot{I}_L \\ \dot{V}_c \end{bmatrix} = \begin{bmatrix} 0 & -\frac{1-d}{L} \\ \frac{1-d}{C} & -\frac{1}{R_L C} \end{bmatrix} \begin{bmatrix} I_L \\ V_c \end{bmatrix} + \begin{bmatrix} \frac{1}{L} \\ 0 \end{bmatrix} V_{FC} \tag{14}$$

$$\begin{bmatrix} V_o \\ I_{FC} \end{bmatrix} = \begin{bmatrix} 0 & 1 \\ 1 & 0 \end{bmatrix} \begin{bmatrix} I_L \\ V_c \end{bmatrix} \tag{15}$$

B. 3-ϕ DC-AC Inverter

The power circuit of 3-ϕ DC-AC inverter with output LC filter considered in this paper is shown in Fig. 4.

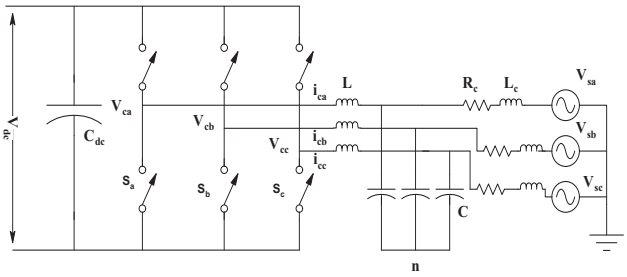

Fig. 4. 3-ϕ DC-AC inverter with LC filter interfacing inductor

The 3-ϕ voltage on the input side (V_{ca}, V_{cb}, V_{cc}) can be expressed in terms of V_{dc} and switching function state of ON/OFF status of device of each leg (S_a, S_b, S_c) as,

$$V_{ca} = \frac{V_{dc}}{3}(2S_a - S_b - S_c) \tag{16}$$

$$V_{cb} = \frac{V_{dc}}{3}(-S_a + 2S_b - S_c) \tag{17}$$

$$V_{cc} = \frac{V_{dc}}{3}(-S_a - S_b + 2S_c) \tag{18}$$

C. LC Filter

To reduce the harmonics in voltage and current, LC filter is used. The cut-off frequency of LC filter is represented as,

$$f = \frac{1}{2\pi\sqrt{LC}} \tag{19}$$

IV. Control of Power Conditioning Unit

In the multi-staged PCU used for fuel cell distributed generation system, the DC-DC converter is controlled using hysteresis controller whereas the 3-ϕ DC-AC inverter is controlled using adaptive hysteresis control.

A. Hysteresis Control of DC-DC Converter

Hysteresis voltage mode control is the simplest and most intuitive control strategy for DC-DC converter as it don't require a compensation network. The comparator which compares the output DC voltage with the reference DC voltage has a small amount of hysteresis denoted by ϵ. The switch of the DC-DC converter is switched ON when output voltage drops below $V_{ref} - \epsilon$ and the switch is turned ON, when the output voltage exceeds $V_{ref} + \epsilon$

The block diagram of hysteresis control of DC-DC converter is shown in Fig. 5.

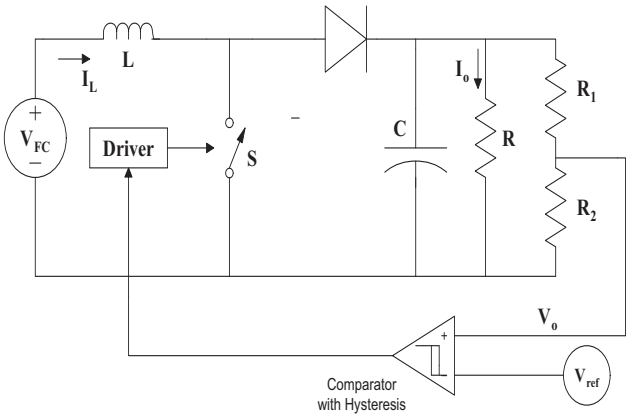

Fig. 5. Hysteresis Control of Boost Converter

B. Hysteresis Control of DC-AC Inverter

There are numerous pulse width modulation schemes available in literature and the survey of some of the schemes are available in [21], [22]. Hysteresis current controller (HCC) is one of the nonlinear control techniques widely used for control of voltage source inverter (VSI) because of its stability, accuracy and faster response. In the HCC the error function is centered in a preset hysteresis band. When the error exceeds the upper or lower hysteresis limit the controller makes an appropriate switching decision to control the error within the hysteresis band and send these pulses to VSI to produce the reference current. The hysteresis band control scheme is shown in Fig. 6.

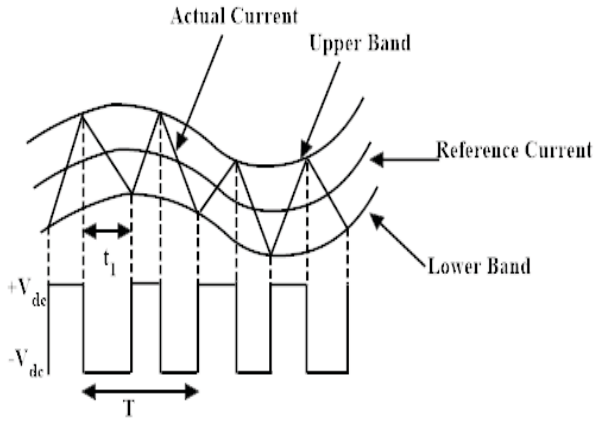

Fig. 6. Hysteresis Band Control

C. Adaptive HCC of DC-AC Inverter

Despite several advantages there are some limitations of HCC as it generates uneven switching frequency which causes problem in control. Therefore adaptive hysteresis based current controller technique is proposed in [23], [24]. In adaptive hysteresis based current controller, the hysteresis band is a function of load profile and changes according to the load. When the current error exceeds the upper limit of the adaptive-hysteresis band, the lower switch is turned ON. If the error current crosses the lower limit of the adaptive-hysteresis band, the upper switch is turned ON. Hence,the actual current is forced to track the reference current within the hysteresis-band. Fig. 7 illustrates the block diagram of adaptive HCC technique.

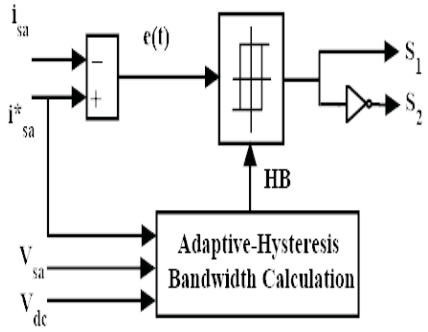

Fig. 7. Block diagram of Adaptive HCC

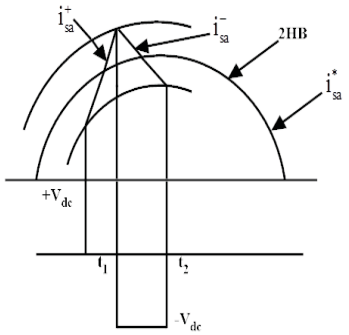

Fig. 8. Current and Voltage in Hysteresis Band

For time interval t_1 and t_2, the following equations can be written

$$\frac{di^+_{sa}}{dt} = \frac{1}{L}(V_{dc} - v_s) \tag{20}$$

$$\frac{di^-_{sa}}{dt} = -\frac{1}{L}(V_{dc} + v_s) \tag{21}$$

Here L is the phase inductance, $\frac{di^+_{sa}}{dt}$ and $\frac{di^-_{sa}}{dt}$ are the rising and falling current segment respectively. From the geometry of Fig. 8, the following equations can be written in the hysteresis-band curvature with respective switching intervals

$$\frac{di^+_{sa}}{dt}t_1 - \frac{di^*_{sa}}{dt}t_1 = 2HB \tag{22}$$

$$\frac{di^-_{sa}}{dt}t_2 - \frac{di^*_{sa}}{dt}t_2 = -2HB \tag{23}$$

$$t_1 + t_2 = T_C = \frac{1}{f_c}$$

f_c is the switching frequency.
Adding (22) and (23) ,

$$\frac{di_{sa}^{+}}{dt}t_1 + \frac{di_{sa}^{-}}{dt}t_2 - \frac{di_{sa}^{*}}{dt}\frac{1}{f_c} = 0 \tag{24}$$

Substituting the values

$$\frac{(V_{dc} - v_s)}{L}t_1 - \frac{(V_{dc} + v_s)}{L}t_2 - \frac{di_{sa}^{*}}{dt}\frac{1}{f_c} = 0 \tag{25}$$

$$\frac{(V_{dc} - v_s)}{L}t_1 - \frac{(V_{dc} + v_s)}{L}t_2 - \frac{di_{sa}^{*}}{dt}\frac{1}{f_c} = 0 \tag{26}$$

$$t_1 - t_2 = \frac{L}{V_{dc}f_c}\left(\frac{v_s}{L} + \frac{di_{sa}^{*}}{dt}\right) \tag{27}$$

Subtracting (22) and (23) ,

$$\frac{di_{sa}^{+}}{dt}t_1 - \frac{di_{sa}^{-}}{dt}t_2 - \frac{di_{sa}^{*}}{dt}(t_1 - t_2) = 4HB \tag{28}$$

$$\frac{(V_{dc} - v_s)}{L}t_1 + \frac{(V_{dc} + v_s)}{L}t_2 - \frac{di_{sa}^{*}}{dt}(t_1 - t_2) = 4HB \tag{29}$$

$$\frac{V_{dc}}{L}(t_1 + t_2) - \frac{v_s}{L}(t_1 - t_2) - \frac{di_{sa}^{*}}{dt}(t_1 - t_2) = 4HB \tag{30}$$

$$HB = \frac{1}{4}\left[\frac{V_{dc}}{f_cL} - \frac{L}{V_{dc}f_c}\left(\frac{v_s}{L} + \frac{di_{sa}^{*}}{dt}\right)^2\right] \tag{31}$$

$$HB = \frac{V_{dc}}{4f_cL}\left[1 - \frac{L^2}{V_{dc}^2}\left(\frac{v_s}{L} + m\right)^2\right] \tag{32}$$

V. Simulation Results

Simulation of multi-staged PCU based fuel cell distributed generation system has been carried out in MATLAB/Simulink. A SOFC stack is considered which provides an unregulated output voltage of 200 V DC. To regulate and boost up the DC voltage a simple DC-DC boost converter is used. Hysteresis voltage mode control is used to control the output voltage of the converter. Boost converter and hysteresis voltage mode control is considered because of its lower part count and simple architecture. With the help of DC-DC boost converter and voltage mode hysteresis controller the unregulated voltage of fuel cell stack is boosted to an average value of 440 V DC. To generate utility AC signal, boost converter is connected with a 3-ϕ VSI and adaptive hysteresis controller is used to control the inverter. The harmonics in the output signal is filtered out using LC filter so the filtered output is purely sinusoidal in nature.

A. Power Quality

The output voltage provided by the fuel cell distributed generation system must have low harmonic contents. The harmonic content must not exceed the stipulated limit provided by the international standards such as IEEE 519-1992, IEC 61000-3-2, IEC 1000-3-2 and IEC 1000-3-4.

Distorted waveform of voltage and current can be represented in terms of fourier series as

$$v(t) = \sum_{h=1}^{\infty} \sqrt{2}V_h \sin(h\omega_o t + \theta_h) \tag{33}$$

$$i(t) = \sum_{h=1}^{\infty} \sqrt{2}I_h \sin(h\omega_o t + \theta_h) \tag{34}$$

Here, V_h and I_h are RMS values of h^{th} order harmonic.
The power quality is measured in terms of Total Harmonic Distortion (THD). THD calculation for voltage and current is represented as

$$THD_V = \frac{\sqrt{\sum_{h=2}^{\infty} V_h^2}}{V_1} \tag{35}$$

$$THD_I = \frac{\sqrt{\sum_{h=2}^{\infty} I_h^2}}{I_1} \tag{36}$$

The simulation parameters are summarized below.

TABLE I
Simulation Parameters

	Parameter	Values
Voltage from Fuel Cell Stack	V_{FC}	200 V DC
Boost Converter	L	49 mH
Boost Converter	C	1400 μF
DC-link Capacitor	C_{dc}	6800 μF
LC filter	L	50 mH
LC filter	C	200 μF
Interfacing Inductance	R_c	1 Ω
Interfacing Inductance	L_c	1 μH

The simulated results for fuel cell based distributed generation system is shown below. Fig. 9 illustrates the fuel cell stack voltage.

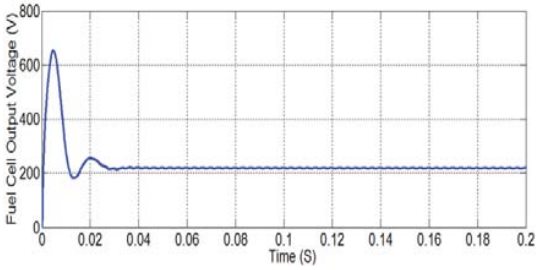

Fig. 9. Output Voltage of Fuel Cell Stack

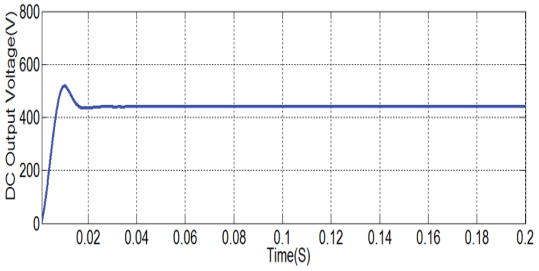

Fig. 10. Output voltage of DC-DC boost converter

Fig. 10 shows the output voltage of DC-DC boost converter. Hysteresis controller provides a stable output voltage despite disturbances. The output current and voltage of 3-ϕ DC-AC

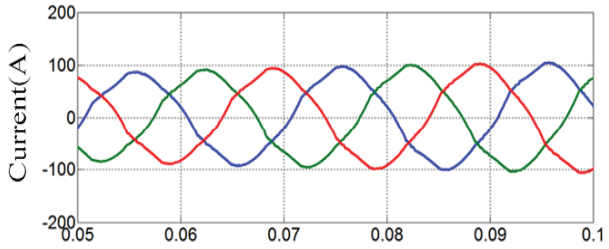

Fig. 11. Output current of inverter

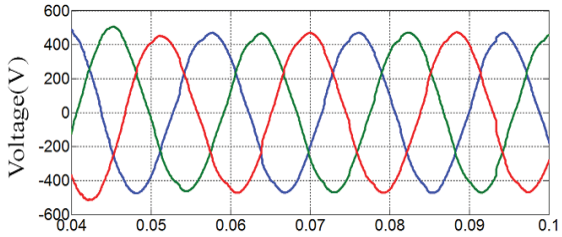

Fig. 12. Output voltage of inverter

inverter is shown in Fig. 11 and Fig. 12 respectively. The adaptive hysteresis controller successfully compensates the effects of any external disturbances.

TABLE II
MEASUREMENT OF TOTAL HARMONIC DISTORTION (THD)

Voltage			Current		
Phase (a)	Phase (b)	Phase (c)	Phase (a)	Phase (b)	Phase (c)
2.1	2.1	2.1	4.5	4.5	4.5

The results in Table II shows that the voltage THD and current THD of fuel cell distributed generation system lies well within the standard limits.

VI. CONCLUSION

This study investigates the effect of hysteresis controller in multi-staged PCU used for fuel cell distributed generation system. Hysteresis controller is used to control the DC-DC boost converter and adaptive hysteresis controller is used to control the 3-ϕ DC-AC inverter. The main purpose of the fuel cell based distributed generation system is to develop such a topology and such a control mechanism which not only provides a perfect grid synchronization but also negates the effect of disturbances due to change in load profile. Adaptive hysteresis controller provides a robust control and efficient load disturbance rejection. The power quality analysis of the distributed generation system is also studied and it remains in between the permissible limits.

REFERENCES

[1] C. Wang, M. Nehrir, and H. Gao, "Control of pem fuel cell distributed generation systems," *IEEE Trans. Energy Convers.*, vol. 21, no. 2, pp. 586–595, 2006.

[2] J.-D. Park and Z. Ren, "Hysteresis-controller-based energy harvesting scheme for microbial fuel cells with parallel operation capability," *IEEE Trans. Energy Convers.*, vol. 27, no. 3, pp. 715–724, 2012.

[3] A. Hajizadeh and M. A. Golkar, "Control of hybrid fuel cell/energy storage distributed generation system against voltage sag," *International Journal of Electrical Power & Energy Systems*, vol. 32, no. 5, pp. 488–497, 2010.

[4] P. Sekhar and S. Mishra, "Sliding mode based feedback linearizing controller for grid connected multiple fuel cells scenario," *International Journal of Electrical Power & Energy Systems*, vol. 60, pp. 190–202, 2014.

[5] J.-C. Wu, K.-D. Wu, H.-L. Jou, Z.-H. Wu, and S.-K. Chang, "Novel power electronic interface for grid-connected fuel cell power generation system," *Energy Conversion and Management*, vol. 71, pp. 227–234, 2013.

[6] A. Sakhare, A. Davari, and A. Feliachi, "Fuzzy logic control of fuel cell for stand-alone and grid connection," *Journal of Power Sources*, vol. 135, no. 1, pp. 165–176, 2004.

[7] A. Kirubakaran, S. Jain, and R. Nema, "A two-stage power electronic interface for fuel cell-based power supply system," *Int. J. Power Electron.*, vol. 3, no. 2, pp. 111–133, 2011.

[8] A. Gebregergis, P. Pillay, D. Bhattacharyya, and R. Rengaswemy, "Solid oxide fuel cell modeling," *IEEE Trans. Ind. Electron.*, vol. 56, no. 1, pp. 139–148, 2009.

[9] D. J. Hall and R. G. Colclaser, "Transient modeling and simulation of a tubular solid oxide fuel cell," *IEEE Trans. Energy Convers.*, vol. 14, no. 3, pp. 749–753, 1999.

[10] J. Padulles, G. Ault, and J. McDonald, "An integrated sofc plant dynamic model for power systems simulation," *Journal of Power sources*, vol. 86, no. 1, pp. 495–500, 2000.

[11] F. Jurado, "Modeling sofc plants on the distribution system using identification algorithms," *Journal of power sources*, vol. 129, no. 2, pp. 205–215, 2004.

[12] S. Kakac, A. Pramuanjaroenkij, and X. Y. Zhou, "A review of numerical modeling of solid oxide fuel cells," *International journal of hydrogen energy*, vol. 32, no. 7, pp. 761–786, 2007.

[13] R. Bove and S. Ubertini, "Modeling solid oxide fuel cell operation: Approaches, techniques and results," *Journal of Power Sources*, vol. 159, no. 1, pp. 543–559, 2006.

[14] M. Hussain, X. Li, and I. Dincer, "Mathematical modeling of planar solid oxide fuel cells," *Journal of Power Sources*, vol. 161, no. 2, pp. 1012–1022, 2006.

[15] B. Huang, Y. Qi, and M. Murshed, "Solid oxide fuel cell: Perspective of dynamic modeling and control," *Journal of Process Control*, vol. 21, no. 10, pp. 1426–1437, 2011.

[16] F. Blaabjerg, Z. Chen, and S. B. Kjaer, "Power electronics as efficient interface in dispersed power generation systems," *IEEE Trans. Power Electron.*, vol. 19, no. 5, pp. 1184–1194, 2004.

[17] A. Kirubakaran, S. Jain, and R. Nema, "A review on fuel cell technologies and power electronic interface," *Renewable and Sustainable Energy Reviews*, vol. 13, no. 9, pp. 2430–2440, 2009.

[18] J. M. Carrasco, L. G. Franquelo, J. T. Bialasiewicz, E. Galván, R. P. Guisado, M. A. Prats, J. I. León, and N. Moreno-Alfonso, "Power-electronic systems for the grid integration of renewable energy sources: A survey," *IEEE Trans, Ind. Electron.*, vol. 53, no. 4, pp. 1002–1016, 2006.

[19] J. Andújar, F. Segura, E. Durán, and L. Rentería, "Optimal interface based on power electronics in distributed generation systems for fuel cells," *Renewable Energy*, vol. 36, no. 11, pp. 2759–2770, 2011.

[20] F. Blaabjerg, R. Teodorescu, M. Liserre, and A. V. Timbus, "Overview of control and grid synchronization for distributed power generation systems," *IEEE Trans. Ind. Electron.*, vol. 53, no. 5, pp. 1398–1409, 2006.

[21] J. Holtz, "Pulsewidth modulation for electronic power conversion," *Proceedings of the IEEE*, vol. 82, no. 8, pp. 1194–1214, 1994.

[22] M. P. Kazmierkowski and L. Malesani, "Current control techniques for three-phase voltage-source pwm converters: a survey," *IEEE Trans. Ind. Electron.*, vol. 45, no. 5, pp. 691–703, 1998.

[23] B. K. Bose, "An adaptive hysteresis-band current control technique of a voltage-fed pwm inverter for machine drive system," *IEEE Trans. Ind. Electron.*, vol. 37, no. 5, pp. 402–408, 1990.

[24] M. Kale and E. Ozdemir, "An adaptive hysteresis band current controller for shunt active power filter," *Electric power systems research*, vol. 73, no. 2, pp. 113–119, 2005.